Available online at www.sciencedirect.com
ScienceDirect
Journal of the European Ceramic Society 27 (2007) 4313–4320
www.elsevier.com/locate/jeurceramsoc

# Admittance and dielectric spectroscopy of polycrystalline semiconductors

Paulo R. Bueno *, José A. Varela, Elson Longo

*Universidade Estadual Paulista, Instituto de Química, Departamento de Físico-Química, P.O. Box 355, 14800-900, Araraquara, São Paulo, Brazil*

Available online 29 March 2007

**Abstract**

This text discusses about advantageous, powerful and limitations of admittance and dielectric spectroscopy in the characterization of polycrystalline semiconductors. In the context of polycrystalline semiconductors or dielectric materials, the admittance or dielectric frequency response analyses are shown to be sometimes more useful than impedance spectra analysis, mainly because information on the capacitances or deep trap states are possible to be monitored from admittance or dielectric spectra as a function of dopant concentration or annealing effects. The majority of examples of the application of admittance or dielectric analysis approach were here based on $SnO_2$- and ZnO-based polycrystalline semiconductors devices presenting nonohmic properties. Examples of how to perform the characterization of Schottky barrier in such devices are clearly depicted. The approach is based on findings of the "true" Mott-Schottky pattern of the barrier by extracting the grain boundary capacitance value from complex capacitance diagram analysis. The equivalent circuit of such kind of devices is mainly consistent with the existence of three parallel elements: the "high-frequency" limit related to grain boundary capacitances, the complex incremental capacitance at intermediate frequency related to the deep trap relaxation and finally at low frequency region the manifestation of the conductance term representing the dc conductance of the multi-junction device.


*Keywords:* Impedance spectroscopy; Varistor

## 1. Introduction

Impedance spectroscopy (IS) is the most popular frequency response technique applied to unravel the complexities involved in electroceramic materials.[1–3] A lot of information can be obtained from this technique which are very useful to reveal the relationship between electrical properties and the physical chemistry features involved in the preparation of the materials, such as microstructure formation and features, composition, dopant and/or defect distribution, etc.[1–3] This technique is largely applied in the studies of polycrystalline ceramic solid electrolytes for the calculation of transport numbers, concentration of carriers, charge-carrying species separation, electronic and ionic defect amount and their mobility.[1] The influence of oxygen partial pressure, dopant concentration, impurities and second phase precipitation are also usually probed by this technique. As the solid electrolytes of practical importance are frequently polycrystalline, bulk and grain boundary conductivities are also taken into account and its separation is of special interest.[3]

In the case of solid electrolytes the conductive term dominates the frequency response and then impedance diagram representation and interpretation (traditionally known as impedance spectroscopy) is most useful than other kinds of frequency response representation of the systems under study.[3]

Alternatively to the solid state electrolytes, another example of electroceramic devices that present polycrystalline nature is the voltage-dependent resistors which are ceramic materials that do not obey the Ohm's law.[4–7] They are comprised of metal oxides and are also referred as varistor devices.[8,9] All of metal oxide varistor systems are polycrystalline materials or devices comprised of a semiconducting matrix of band gap energy around 3 eV (ZnO, $TiO_2$, $SnO_2$ and $SrTiO_3$).[8,9] The nonohmic properties of such devices are related to the potential barrier formation at grain boundary whose main conduction characteristic is dominated by electronic tunneling over the barrier at ambient temperature.[8,9] The barrier nature is considered to be of Schottky-type barrier.[8,10] Due to the polycrystalline morphology these barriers are modeled as double Schottky-type

* Corresponding author.
*E-mail address:* prbueno@iq.unesp.br (P.R. Bueno).

0955-2219/$ – see front matter © 2007 Elsevier Ltd. All rights reserved.
doi:10.1016/j.jeurceramsoc.2007.02.155

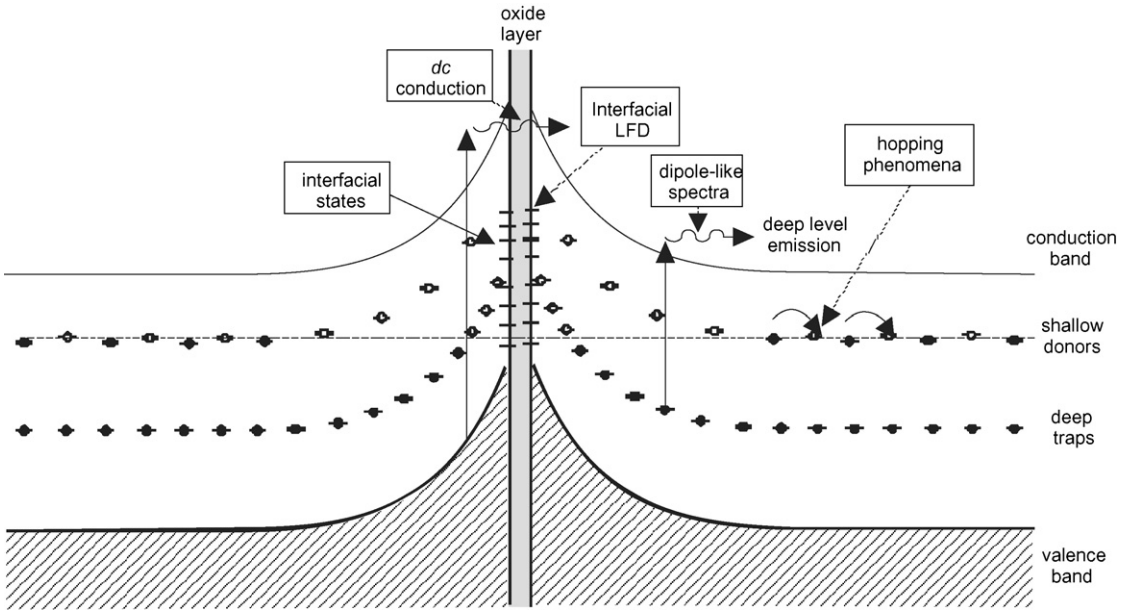


Fig. 1. Representation of an individual double Schottky barrier junction for a metal oxide polycrystalline semiconductors possessing nonohmic behavior. The specific case of segregated oxide metal or precipitated oxide phase layer is shown. The picture is applicable to a variety of metal oxide polycrystalline semiconductor systems. In this figure possible phenomena that interfere on the frequency response analysis are shown, although some of than were not investigated in the present text. Due to the polycrystalline nature of systems, these phenomena are very difficult to be studied in detail (examples are the hopping conductivity and interfacial low frequency dispersion—LFD).

over grain boundary region or junctions between two different grains (see Fig. 1).[8,10,11]

In the later kind of device considered, IS technique is also applied to explore the differences between bulk and grain boundary resistance contribution to the overall resistive response.[3] However, the properties of the grain boundary are rarely fully explored in the correct context of Schottky-type barrier. This occurs particularly because grain boundaries are considered to possess solely one type of charge contributing to its overall capacity. This approach is not correct in the context of polycrystalline semiconductor as shall be demonstrated here. An additional relaxation process exit in the grain boundary region due to the grain semiconductor nature (e.g. deep trap states existing in the grain) and then impedance diagram representation is less useful than other kind of frequency response representation to separate different grain boundary charges contribution to the overall capacitance of this region, mainly if frequency response measurements are taken at room temperature.[11] Therefore, to deal with such capacitive additional term, or additional relaxation process, admittance or dielectric complex diagrams representation of frequency response is more useful than the impedance complex representation.[10–14] This lead to the definition of admittance spectroscopy (AS) and dielectric spectroscopy (DS) that are, respectively, based on admittance and dielectric functions, respectively. Admittance or dielectric functions are impedance-related functions and the differences between them are just related to its weighting with frequency.[3,10–12,14]

Therefore, the main goal of this work is to demonstrate that the use of AS and/or DS in the context of polycrystalline semiconductor is more useful than the use of IS. In other words, the purpose is to demonstrate that the admittance and/or dielectric complex diagrams of the frequency response of polycrystalline semiconductor is more useful than the impedance diagrams to reveal the relaxation processes, electrical conduction mechanism and charge accumulation involved with grain boundaries, at least in the case of highly dense polycrystalline devices. The influence of the porosity or number of active barrier in the global response will be also considered and discussed. Indeed, for this purpose we will mainly restrict our examples to polycrystalline nonohmic devices comprised of $SnO_2$ and ZnO matrix.[10–12,14] However, there are a lot of other semiconductor polycrystalline systems in which the approach presented here can be usefully exploited.[15]

## 2. Admittance and dielectric complex functions

In the context of junction devices, of which polycrystalline semiconductors is a multi-junction systems class, AS is essentially synonymous of DS. However, it is very important to mention that the dielectric behavior of semiconductors is not usually regarded as a part of the science of dielectrics.[16]

The reason of why AS is considered as essentially synonymous of DS in the semiconductor junctions context is based on the fact that the admittance functions ($Y^*(\omega) = Y' + jY''$ in which $\omega = 2\pi f$ is the angular frequency and $j = \sqrt{-1}$) is directly proportional to the capacitance function according to

$$C^*(\omega) = (j\omega)^{-1} Y(\omega), \quad (1)$$

$$C^*(\omega) = \left(\frac{Y''}{\omega} - \frac{jY'}{\omega}\right) = C' + jC'' \quad (2)$$

The real part ($C'$) of the complex capacitance function is related to parallel capacitance ($C' = Y''/\omega = C_p$) while the imaginary part

($C''$) is related to a conductive term ($C'' = Y'/\omega = G_p/\omega$). The $G_p$ (or $G_p/\omega$) conductive term is a parameter that includes the dc conductance and other relaxation-associated loss as shall be commented later herein.

## 3. Equivalent circuit representation

As already commented previously, the admittance or dielectric response of the polycrystalline semiconductors depends on the bulk (grain) and grain boundary responses.[16] As in the special case to be described here of nonohmic polycrystalline semiconductor devices, the general equivalent circuit representation of the response (without consider the electrodes or contacts) is shown in Fig. 2.[10–12,14] On the one hand, the $R_g$ and $C_g$ stands for resistance and capacitance of grain or bulk, respectively. On the other hand, $R_{gb}$ and $C_{gb}$ stands for resistance and capacitance of grain boundary. The additional relaxation impedance shown in Fig. 2 stands for an additional relaxation process related to excitation from deep traps existing into the band gap and the corresponding reverse capture processes. There are three possibilities for this kind of relaxation: (a) ideal transitions or rate dynamics of trapping and detrapping represented by a Debye-like process,[17] (b) distributed rate dynamics with transitions represented by Cole–Cole-like pattern[17] and finally a more general function (c) which is known as Havriliak–Negami relaxation function.[17] This relaxation function on the context of semiconductor junctions represents distributed dynamics of trapping allied to interactions between charges, i.e. trapping/detrapping dynamics influenced by charge interactions on the conductance band or trapping state.[18] The details of the dynamics are still not completely understood.

The relaxations from (a) to (c) are represented, respectively, by the following functions:

$$C^*(\omega) = C_{gb} + \frac{C_t - C_{gb}}{1 + (j\omega\tau)}, \quad (3)$$

$$C^*(\omega) = C_{gb} + \frac{C_t - C_{gb}}{1 + (j\omega\tau)^{1-\alpha}}, \quad (4)$$

$$C^*(\omega) = C_{gb} + \frac{C_t - C_{gb}}{(1 + (j\omega\tau)^{1-\alpha})^{\beta}}. \quad (5)$$

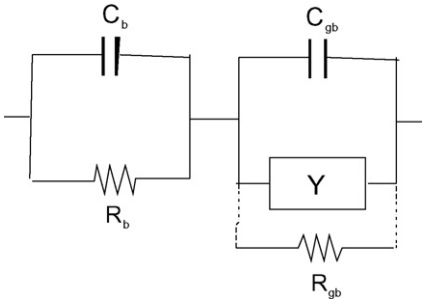


Fig. 2. General equivalent circuit representation of polycrystalline semiconductors. It is important to note that the semiconductor nature of the polycrystalline material is related to the $Y$ admittance or impedance element and according to the nature of deep trap states it can be represented by one of the relaxation functions of Eqs. (3)–(5).

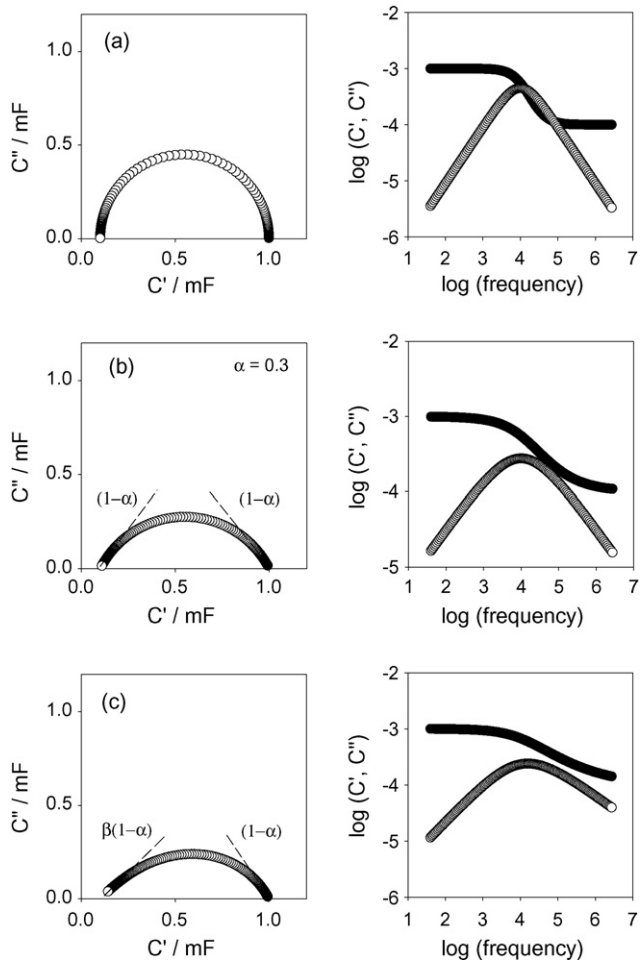


Fig. 3. Complex capacitance and Bode capacitive diagrams of relaxation processes related, respectively, to Eqs. (3)–(5). (a) Debye relaxation process, (b) Cole–Cole relaxation with $\alpha = 0.3$ and (c) Havriliak–Negami relaxation with $\alpha = 0.3$ and $\beta = 0.7$.

in which $0 < \alpha < 1$. Note that when $\alpha = 0$ and $\beta = 1$, the Eq. (5) reduces to Eq. (3). Therefore, Eq. (5) is a general relaxation function that contains both Eqs. (3) and (4). Fig. 3 shows the complex capacitance diagrams representation of such kind of relaxations. In Eqs. (3)–(5), $C_{gb}$ is the capacitance of grain boundary as already named, $C_t$ is the capacitance of deep trap state and $\tau$ is the trapping/release relaxation time.

It is important to point out that albeit Eqs. (3)–(5) are used in dielectric interpretation of the dipolar relaxation,[18] in the present context it is representing the electronic transitions at barrier occurring in the junctions of a polycrystalline system. Therefore, physically the context is totally different. Based on this aspect, it is also important to stress that in the present discussion of dielectric properties of a multi-junction barrier system, it is not appropriate to talk about material parameters such as dielectric permittivity or susceptibility since it is almost impossible to have sufficient knowledge of the geometry, i.e. of the thickness of the region in question (grain boundary) to determine the former. Therefore, it is most convenient express the response in terms of complex capacitance ($C^*$) instead of complex dielectric form ($\varepsilon^*$).

## 4. Schottky-like grain boundary junctions

The applications of AS or DS to polycrystalline systems containing Schottky-like grain boundary junctions permit one to obtain all of the mean parameter values related to this kind of junction and to study the influence of specific doping that eventually segregates at grain boundaries among other information as shall be exemplified here.[10,11]

In the context of nonohmic polycrystalline metal oxide, it is firmly established the existence of a double Schottky-like barrier at grain boundaries. In such kind of double Schottky-like barrier the capacitance of grain boundary is related to the bias voltage applied to the junction by the following equation[10,11,13,14,19]:

$$\left(\frac{1}{C_{gb}} - \frac{1}{2C_{gb_0}}\right)^2 = \frac{2p^2}{qk\varepsilon_0 N_d}\left(\phi_b + \frac{V}{p}\right), \quad (6)$$

where $q$ stands for the electron or elementary charge, $k$ the dielectric constant ($k$ to $SnO_2$ grain is ~14), $\varepsilon_0$ the permittivity of free space, $N_d$ the positive space charge density in the depletion layer region (free electron density) and $\phi_b$ is the barrier height. $C_{gb0}$ and $C_{gb}$ are the grain boundary capacitance per unit of area biased, respectively, with zero and $V$ volts. The parameter $p$ is necessary to perform the normalization of the values to the total number of active barrier existing in the polycrystalline systems. So that it is related to the mult-junction features of the system. Obviously, it is a parameter dependent on the microstructure morphology. The $p$ parameter is also one of the major sources of uncertainties on the calculation of the barrier parameter values as shall be discussed further herein.

The density of $N_{IS}$ states at the interface between the grains and the intergranular layer is estimated by using the following relationship:

$$N_{IS} = \left(\frac{2N_d\varepsilon_r\varepsilon_0\phi_b}{q}\right)^{1/2}. \quad (7)$$

## 5. Calculation of grain boundary capacitance and "true" Mott-Schottky pattern

The calculation of $C_{gb}$ separated from other kinds of relaxation processes existing on the grain boundaries, e.g. due to deep trap states, are of special interest to be applied in Eq. (6) to calculate the parameters of the Schottky-type barrier.[10,11,13,14] By using this approach it is possible to calculate the $C$–$V$ or Mott-Schottky pattern of the system. In general, the $C$–$V$ features of polycrystalline system is obtained by using a capacitance value taken in an arbitrarily frequency (which is incorrect and cause errors and misinterpretation of the values). In this case, the capacitance is said to be a frequency-dependent capacitance and the error in the construction of the Mott-Schottky behavior is great so that sometimes it is very difficult to establish any relationship (or correlation) between the parameter values related to the potential barrier (e.g. barrier height, width, etc.) and that related to nonohmic macroscopic parameters (e.g. nonlinear coefficient), which are responsible for the varistor macroscopic electrical properties.

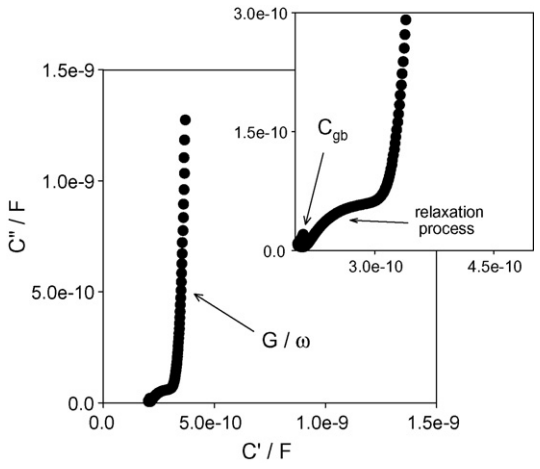


Fig. 4. A typical complex capacitance diagram for $SnO_2$-based polycrystalline semiconductors. At low frequency region, it is observed the conductive term ($G/\omega$) related to the grain boundary resistance. At intermediate frequency, the relaxation process related to the deep trap rate dynamic is shown (better visualized in the inset). Finally, at high frequency region is where the capacitance of grain boundary is obtained separated from other capacitive relaxations.

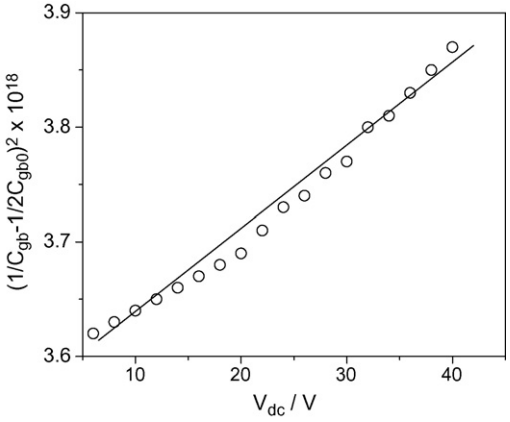


Fig. 5. The "true" Mott-Schottky behavior for $SnO_2$-based varistor system obtained from complex capacitance plane analysis. The frequency is taken in a specific frequency depending on the system, according to approach discussed on the text.

Otherwise, by analyzing the capacitance complex functions response of the system it is possible to obtain the exact or closely value of the $C_{gb}$ separated from other relaxation processes.[10,11] An example is given in Fig. 4, which shows a complex capacitive response of a dense $SnO_2$-based polycrystalline semiconductor presenting a good nonohmic property. The region of frequency where the $C_{gb}$ can be obtained is also indicated in Fig. 4. The relaxation process related to deep trap states is indicated either. This approach leads to the construction of the "true" Mott-Schottky pattern (see Fig. 5) of the polycrystalline system under study.[10,11]

## 6. Calculations of deep trap state energy

Another parameter which could be very useful to explore and analysis in the polycrystalline semiconductor is the deep trap state energy. In the case of frequency response, a small

Table 1
$\alpha$ (Nonlinear coefficient), $E_b$ (breakdown voltage), $v_b$ (voltage per grain), mean grain size ($d$) and relative densities ($\rho_r$) of the SCNCr-X ($SnO_2$.CoO.$Nb_2O_5$.$Cr_2O_3$ −X) varistor systems

| SYSTEM | α | $E_b$ / V.cm$^{-1}$ | $v_b$ / V.grain$^{-1}$ | d / μm | $\rho_r$ / % |
|---|---|---|---|---|---|
| SCNCr-$CeO_2$ | 55 | 5536 | 2.0 | 3.6 | 94.1 |
| SCNCr-$Pr_2O_3$ | 73 | 6110 | 2.4 | 3.9 | 86.8 |
| SCNCr-$La_2O_3$ | 142 | 11525 | 2.3 | 1.9 | 79.7 |

X means $CeO_2$, $Pr_2O_3$ or $La_2O_3$.[11]

ac signal is applied to the boundaries.[11] There is a relaxation when the angular frequency of this ac signal becomes equal to the emission rate $e_n$ of the electrons in a trapping state (see Figs. 1 and 4). Based on the theory of semiconductors it is know that the displacements of the loss peak ($C''(\omega)$) occurs as a function of temperature. The $e_n$ (which is equivalent to $\tau^{-1}$ the time dependence of electron transition) is directly proportional to $\omega_p$ and depends on the temperature as follow[11]:

$$\omega_p = \tau^{-1} = e_n = \sigma_n v_{th} N_c \exp\left[\frac{E_c - E_t}{kT}\right], \quad (8)$$

in which $\omega_p$ is equivalent to $e_n$, $\sigma_n$ the capture cross-section, $v_{th}$ the free-electron thermal velocity, $N_d$ the donor concentration, as already defined previously and, finally, $E_c$–$E_t$ is the energy difference between conduction band and the trapping level.

As the $E_c$–$E_t$ depends on the bulk nature of the polycrystalline device, as expected, it is not influenced by dopants that segregates or precipitates on the grain boundary as shown in Table 2 (Table 1 shows the macroscopic values of nonohmic properties and morphology features). Furthermore, the deep trap state is not influenced by the annealing at different atmospheres, according to Table 3 and also in agreement to the atomic model defect proposed to control the grain boundary composition.[20] More details will be given on the next section.

## 7. Examples of applications in nonohmic devices

The main goal of this section is to present examples of applications of the approaches described in the previous sections. Accordingly, Table 2 presents some potential barrier parameter values obtained in $SnO_2$-based varistor (nonohmic device) systems. It is possible to study the influence of the additions of three different dopants on the potential barrier parameter values, as demonstrated in Table 2.[11] From transmission electronic microscopy (TEM) analysis, it was concluded that all of these dopants influences the grain boundary region by segregation and precipitation.[21,22] Table 1 shows information for the $SnO_2$-based polycrystalline semiconductor systems concerning nonohmic properties and microstructure characteristics.[10]

From the comparison between both tables it is possible to observe the tendency of increasing of the barrier height as the nonlinear coefficient (which defines the quality of the nonohmic properties) increases. However, although the observed tendency is correct, the values of barrier height for systems containing $Pr_2O_3$ and $La_2O_2$ are overestimated. This overestimation is related to the miscalculation of $p$ parameter in Eq. (6). The calculation of the value of the $p$ parameter is based on the mean grain size and on the distance from electrodes or, in other words, depends on the thickness of the sample. A miscalculation of $p$ parameter value is, e.g. introduced by porosity or the existence of a large number of nonactive potential barriers. The influence of the amount of nonactive potential barrier is easier to be considered as shall be demonstrated in the next section. However, the effect of porosity is more difficult to be considered and corrected. In Table 2, the values of barrier height are most overestimated due to porosity effect (see the values of relative density of the samples) instead of the amount of nonactive potential barriers.

Table 2
$\phi_b$ (Potential barrier height), $N_d$ (represents the donor concentration), $N_{IS}$ (interfacial density of states) and $\delta$ (barrier width) values for a back-to-back Schottky-type potential barrier of SCNCr-X varistor systems. The shading values in this Table is are values over estimated due to relative densities (see shading values of Table 1)

| SYSTEM | $\phi_b$ / eV | $N_d$ (x 10$^{23}$) / m$^{-3}$ | $N_{IS}$ (x 10$^{16}$) / m$^{-2}$ | δ / nm | $E_c - E_t$ / eV |
|---|---|---|---|---|---|
| SCNCr-$CeO_2$ | 1.10 ± 0.05 | 7.79 | 3.64 | 23.4 | 0.43 ± 0.02 |
| SCNCr-$Pr_2O_3$ | 1.99 ± 0.04 | 5.76 | 4.21 | 36.5 | 0.41 ± 0.03 |
| SCNCr-$La_2O_3$ | 2.48 ± 0.06 | 4.43 x 10$^2$ | 4.12 x 10$^1$ | 4.65 | 0.41 ± 0.02 |

The $\delta$ values were calculated from the electrical neutrality condition ($N_{IS} = 2N_d\delta$). The of potential barrier parameters take into consideration the average number of grains between electrodes ($p$ parameter in Eq. (6) without corrections).[11] Note that the $\phi_b$ values are influenced by porosity (see relative density values in Table 1).

Table 3
$\alpha$, $E_b$, $v_b$ (for nomenclature see Table 1) for the SCNCr-$La_2O_3$ varistor system (relative density around 80%) thermally treated at 900 °C in different atmospheres[11]

| Annealing | $\alpha$ | $E_b$ (V cm$^{-1}$) | $v_b$ (V grain$^{-1}$) |
|---|---|---|---|
| $N_2$-rich atmosphere | 89 | 11,536 | 2.0 |
| $O_2$-rich atmosphere | 145 | 11,831 | 2.3 |

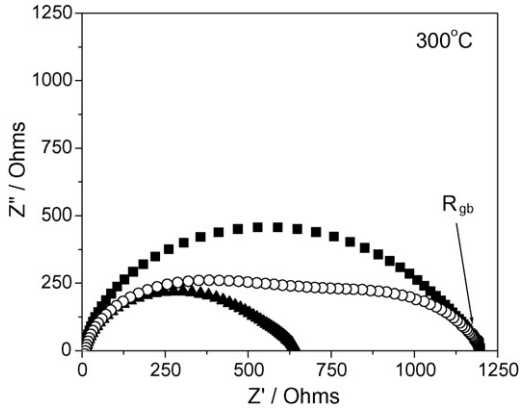


Fig. 6. Complex plane representation of impedance responses for a $SnO_2$.CoO-based varistor system. In this figure, it is possible to observe the reversibility of grain boundary resistance after heat treatments under different atmospheres. (■) As-sintered with nonlinear coefficient (α) ∼32, (▲) $N_2$-with α ∼ 16 and (◯) $O_2$-rich atmosphere with α ∼ 26. Note that the impedance pattern is not totally recovered although the grain boundary resistance value is almost totally recovered.[20].

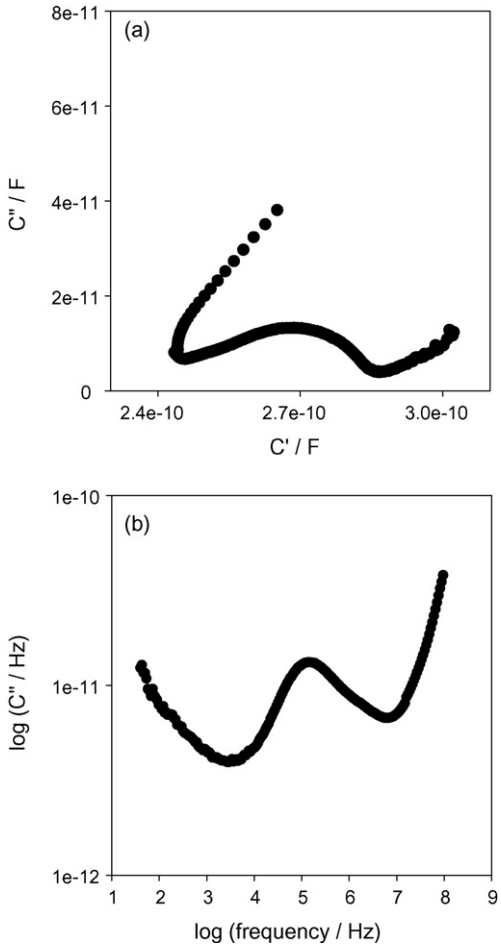


Fig. 7. (a) Complex capacitance diagram of ZnO-based varistor system showing a Havriliak–Negami-like relaxation process for deep trap dynamic. (b) Capacitive loss ($C'' = G/\omega$) diagram.

Table 3 presents the macroscopic values that determine the nonohmic properties. On the other hand, for the same polycrystalline semiconductor system, Table 4 shows the potential barrier parameter values obtained in $SnO_2$-based varistor after annealing at different atmospheres.[20] Again, as foreseen according to the atomic defect model for the Schottky-type barrier formation in polycrystalline semiconductors,[20] the values of potential barrier height rising is accompanied by an increasing of the nonlinear coefficient value which can be showed in Table 3. This observed tendency is correct despite of the fact that the calculated barrier height values are overestimated due to porosity effect that causes an error in the calculation of the $p$ parameter values.

In Fig. 6, it is shown the impedance diagrams of samples after different annealing.[20] As known from literature data the nonlinear coefficient and nonohmic properties decrease tremendously after heat treatments in $N_2$-rich atmosphere.[11,20,23] Nevertheless, the properties can be totally recovered after a new annealing in $O_2$-rich atmosphere. However, albeit the values of the nonlinear coefficient are reversible, the charge distribution on the grain boundary sometimes can be totally rearranged.[11,20,23] Indeed, the parameter of the grain boundary that is totally recovered according to Fig. 6 is the value of $R_{gb}$ and it is one of the most important parameters responsible to the nonlinear coefficient values of the polycrystalline system.

Finally, in Fig. 7, it is possible to observe an admittance response of ZnO-based varistor system.[12–14,24–27] There are some characteristics of admittance response of ZnO-based varistor systems which still deserve some attention and here we illustrate one of them. For instance, the presence of a Havriliak–Negami like distribution for the relaxation of ZnO-based varistor system is commonly observed.[17,27] The origin of such relaxation function in the context of semiconductor junc-

Table 4
$\phi_b$, $N_d$, $N_{IS}$ and $\delta$ (for nomenclature see Table 2) values for a back-to-back Schottky-type potential barrier of the SCNCr-$La_2O_3$ varistor system (relative density around 80%) thermally treated at 900 °C in different atmospheres

| Annealing | $\phi_b$ (eV) | $N_d$ ($\times 10^{23}$) (m$^{-3}$) | $N_{IS}$ ($\times 10^{16}$) (m$^{-2}$) | $\delta$ (nm) | $E_c$–$E_t$ (eV) |
|---|---|---|---|---|---|
| $N_2$-rich atmosphere | 2.27 ± 0.04 | 0.98 | 1.86 | 94.8 | 0.41 ± 0.02 |
| $O_2$-rich atmosphere | 2.57 ± 0.05 | 91.3 | 19.1 | 10.4 | 0.43 ± 0.02 |

These calculations take into account the average number of grains between electrodes ($p$ parameter in Eq. (6) without corrections).[11]

Table 5
Results of nonlinear coefficient ($\alpha$), breakdown electric field ($E_b$), mean barrier height value obtained from the EFM data analysis ($\phi_{efm}$), mean barrier height value obtained by combining Eq. (6) and the complex capacitance plane analysis ($\phi_{conv}$), mean grain size ($d$) obtained for SCNCr ($SnO_2$.CoO.$Nb_2O_5$.$Cr_2O_3$) system[29]

| System | $\alpha$ | $E_b$ (V cm$^{-1}$) | $\phi_{efm}$ (V) | $\phi_{conv}$ (V) | $d$ (μm) |
|---|---|---|---|---|---|
| SCNCr | 75 | 6900 | 1.4 | 1.3 | 2.4 |

tion is still far to be totally understood. Garcia-Belmonte et al.[27] reported that possible changes on the pattern of the distribution can be caused by a more complicated dynamics that could be related to cooperative interactions in disordered media due to higher density of trap states. A detailed study of such distributions is very important in the context of degradation of varistor devices because the mechanism of degradation is considered to be linked to a bulk defect migration phenomena.[27,28]

## 8. Electrostatic force microscopy and admittance spectroscopy

From the pattern of capacitive potential energy obtained from electrostatic force microscopy (EFM) technique as a function of the applied voltage,[29] it is possible to obtain the minimum voltage value corresponding to the mean value of potential barrier height for the active junctions. Such approach was tested in a highly dense $SnO_2$-based polycrystalline semiconductor. Therefore, the value of mean potential barrier height obtained was found to be about 1.4 V.[29] The comparison of this value obtained from EFM with that value obtained from a complex capacitance analysis according to the approach previously discussed is shown in Table 5. The other parameters of the system are still shown in this table, for instance, nonlinear coefficient value and electric breakdown field. The $\phi_{efm}$ and $\phi_{conv}$ are the mean values of potential barrier height obtained by fitting the EFM data and by the methodology of combining Eq. (6) with the complex capacitance analysis, respectively.[29] It is important to emphasize that, for the calculation of $\phi_{conv}$, the $p$ parameter was corrected to consider the 85% of active potential barriers, i.e. $p = 0.85L/d$ ($L$ is the sample thickness and $d$ the mean grain size). The values obtained by using different methodologies were found to be in good agreement.

The amount of 85% of active potential barriers must be the origin of the better correlation obtained between barrier height values and nonohmic properties in metal oxide $SnO_2$-based[29] compared with metal oxide ZnO-based varistors which present an amount of active barrier around 15–35% (because in this last situation the correction of $p$ parameter values is essential). The larger number of active potential barriers in metal oxide-based $SnO_2$ is possibly related to the difficulty in obtaining low voltage varistors of such systems.

## 9. Final remarks and conclusions

It is possible to conclude that admittance or dielectric spectroscopy is a powerful technique to study phenomena occurring in polycrystalline semiconductors. It is very important, from scientific standpoint, in understanding the mechanisms involved in such kind of multi-junction devices. From technological point of view, it can be also used to control and improve devices, mainly because it is a nondestructive technique.

The majority of examples given in this text were based on nonohmic devices, but it is also important to stress that the technique can be useful for any kind of polycrystalline semiconductor. We are at this moment exploring the properties of perovskite-based system possessing nonohmic features allied to huge dielectric properties whose nature is far to be totally understood.[30,31]

## Acknowledgments

The financial support of this research project by the Brazilian research funding agencies CNPq and FAPESP is gratefully acknowledged.

## References

1. Irvine, J. T. S., Sinclair, D. C. and West, A. R., Electroceramics: characterization by impedance spectroscopy. *Adv. Mater.*, 1990, **2**(3), 132–138.
2. Abrantes, J. C. C., Labrincha, J. A. and Frade, J. R., An alternative representation of impedance spectra of ceramics. *Mater. Res. Bull.*, 2000, **35**, 727–740.
3. Macdonald, J. R., *Impedance Spectroscopy*. John Wiley and Sons, New York, 1987.
4. Kim, S.-H., Kim, H.-T., Park, J.-H. and Kim, Y., *I–V* characteristics and impedance spectroscopy of a single grain boundary in Nb-doped SrTiO3. *Mater. Res. Bull.*, 1999, **34**(3), 415–423.
5. Lee, J., Hwang, J.-H., Mashek, J. J., Mason, T. O., Miller, A. E. and Siegel, R. W., Impedance spectroscopy of grain boundaries in nanophase ZnO. *J. Mater. Res.*, 1995, **10**(9), 2295–2300.
6. Smith, A., Baumard, J.-F., Abélard, P. and Denanot, M.-F., AC impedance measurement and *V–I* characteristics for Co-, Mn-, or Bi-doped ZnO. *J. Appl. Phys.*, 1989, **65**(12), 5119–5125.
7. Viswanath, R. N. and Ramasamy, S. N., Impedance spectroscopy studies of nanostructured ZnO based varistor materials. *Mater. Trans.*, 2001, **42**(8), 1647–1652.
8. Clarke, D. R., Varistor ceramics. *J. Am. Ceram. Soc.*, 1999, **82**(3), 485–502.
9. Gupta, T., Application of zinc oxide varistors. *J. Am. Ceram. Soc.*, 1990, **73**, 1817–1840.
10. Bueno, P. R., Cassia-Santos, M. R., Leite, E. R., Longo, E., Bisquert, J., Garcia-Belmonte, G. *et al.*, Nature of the Schottky type barrier of hyghly dense $SnO_2$ systems displaying nonohmic behaviour. *J. Appl. Phys.*, 2000, **88**(11), 6545–6548.
11. Bueno, P. R., Oliveira, M. M., Bacelar-Junior, W. K., Leite, E. R., Longo, E., Garcia-Belmonte, G. *et al.*, Analysis of the admittance-frequency and capacitance–voltage of dense $SnO_2$·CoO-based varistor ceramics. *J. Appl. Phys.*, 2002, **91**(9), 6007–6014.
12. Alim, M. A., An analysis of the Mott-Shottky behavior in ZnO-$Bi_2O_3$ based varistors. *J. Appl. Phys.*, 1995, **78**, 4776–4779.
13. Alim, M. A., Seitz, M. A. and Hirthe, R. W., Complex plane analysis of trapping phenomena in zinc oxide based varistor grain boundaries. *J. Appl. Phys.*, 1988, **63**, 2337–2345.
14. Alim, M. A., Admittance-frequency response in zinc oxide varistor ceramics. *J. Am. Ceram. Soc.*, 1989, **72**, 28–32.
15. Jonscher, A. K., The "universal" dielectric response. *Nature*, 1977, **267**, 673.
16. Jonscher, A. K., Dielectric characterisation of semiconductors. *Solid-State Electron.*, 1990, **33**, 737–742.
17. Böttcher, C. J. F. and Bordewijk, P., *Theory of Electric Polarization. Dielectric in Time-Dependent Fields*, *vol. II*. Elsevier, Amsterdam, 1992.

18. Jonscher, A. K., *Universal Relaxation Law*. Chelsea Dielectric Press, London, 1996.
19. Mukae, K., Tsuda, K. and Nagasawa, I., Capacitance versus voltage characteristics of ZnO varistors. *J. Appl. Phys.*, 1979, **50**, 4475–4476.
20. Bueno, P. R., Leite, E. R., Oliveira, M. M., Orlandi, M. O. and Longo, E., Role of oxygen at the grain boundary of metal oxide varistors: a potential barrier formation mechanism. *Appl. Phys. Lett.*, 2001, **79**(1), 48–50.
21. Oliveira, M. M., Soares Jr., P. C., Bueno, P. R., Leite, E. R., Longo, E. and Varela, J. A., Grain-boundary segregation and precipitates in $La_2O_3$ and $Pr_2O_3$ doped $SnO_2$·CoO-based varistors. *J. Eur. Ceram. Soc.*, 2003, **23**, 1875–1880.
22. Oliveira, M. M., Bueno, P. R., Longo, E. and Varela, J. A., Influence of $La_2O_3$, $Pr_2O_3$ and $CeO_2$ on the nonlinear properties of $SnO_2$ multicomponent varistor. *Mater. Chem. Phys.*, 2002, **74**, 150–153.
23. Santos, M. R. S., Bueno, P. R., Longo, E. and Varela, J. A., Effect of oxidizing and reducing atmospheres on the electrical properties of dense $SnO_2$-based varistors. *J. Eur. Ceram. Soc.*, 2001, **21**, 161–167.
24. Alim, M. A., High-frequency terminal resonance in ZnO-$Bi_2O_3$-based varistors. *J. Appl. Phys.*, 1993, **74**, 5850–5853.
25. Alim, M. A. and Seitz, M. A., Singular nature of preferential conducting paths at high electric field in ZnO-based varistor. *J. Am. Ceram. Soc.*, 1988, **71**(5), C246–C249.
26. Alim, M. A., Seitz, M. A. and Hirthe, R. W., High-temperature/field alternating-current behavior of ZnO-based varistor. *J. Am. Ceram. Soc.*, 1988, **71**(1), C52–C55.
27. Garcia-Belmonte, G., Bisquert, J. and Fabregat-Santiago, F., Effect of trap density on the dielectric response of varistor ceramics. *Solid-State Electron.*, 1999, **43**, 2123–2127.
28. Takata, M., Relationship between degradation phenomenon and trap levels in a ZnO varistor. *Am. Ceram. Soc. Bull.*, 1993, **72**(5), 96–98.
29. Vasconcelos, J. S., Vasconcelos, N. S. L. S., Orlandi, M. O., Bueno, P. R., Varela, J. A., Longo, E. *et al.*, Electrostatic force microscopy as a tool to estimate the number of active potential barriers in dense non-ohmic polycrystalline SnO2 devices. *Appl. Phys. Lett.*, 2006, **89**, 152102–152105.
30. Bueno, P. R., Orlandi, M. O., Simões, L. G. P., Leite, E. R., Longo, E. and Cerri, J. A., Non-ohmic behavior of $SnO_2$-MnO Polycrystalline Ceramics. Part I. Correlations between microstructural morphology and non-ohmic features. *J. Appl. Phys.*, 2004, **96**, 2693.
31. Bueno, P. R., Ramírez, M. A., Varela, J. A. and Longo, E., Dielectric spectroscopy analysis of $CaCu_3Ti_4O_{12}$ polycrystalline systems. *Appl. Phys. Lett.*, 2006, **89**, 191117–191119.